

Cultured Myoblasts Orientation under Couette Type of Shear Flow between Parallel Disks: Fusion and Division

Yuji ENDO, Shigehiro HASHIMOTO, Sora TOMA, Akira ASAHINO

Biomedical Engineering, Department of Mechanical Engineering, Kogakuin University

Tokyo, 163-8677, Japan

<http://www.mech.kogakuin.ac.jp/labs/bio/>

Kiyoshi YOSHINAKA

Health and Medical Research Institute, National Institute of Advanced Industrial Science & Technology

Tsukuba, 305-8564, Japan

ABSTRACT

The effect of shear stress on myoblast has been investigated under the uniform shear flow *in vitro*. The culture medium was sandwiched with a constant gap between a lower stationary culture plate and an upper rotating parallel plate to make a Couette type of shear flow. The wall shear stress (τ) on the lower culture disk was controlled by the rotating speed of the upper disk. C2C12 (mouse myoblast cell line) was used in the test. After cultivation without flow for 24 hours for adhesion of cells on the lower plate, τ was continuously applied on cells for 7 days in the incubator. The behavior of each cell was traced at the time-lapse image observed by an inverted phase contrast microscope placed in an incubator. The experimental results show that cells make both division and fusion under shear stress < 2 Pa. Interaction between divided cells decreases with the distance between cells. The smaller cell tends to follow the bigger cell related to the alignment.

Keywords: Biomedical Engineering, Shear Stress, C2C12, Orientation, Division and Fusion.

1. INTRODUCTION

The effect of the shear flow on the endothelial cells, which are exposed to the blood flow on the inner surface of the vessel wall, were investigated in many studies [1–10]. In the previous study with the vortex flow [11] by the swinging plate *in vitro*, C2C12 (mouse myoblast cell line) made orientation perpendicular to the direction of the flow, although HUVEC (human umbilical vein endothelial cell) made orientation along the streamline of the flow [12]. The orientation of each cell in the tissue depends on that of neighbor's cell. To analyze the mechanism of making orientation of cells, the behavior of each cell in the shear flow field should be quantitatively observed during tissue making.

At the wall shear stress, a cell shows the following responses: deformation [1–3], rotation [4, 5], migration [6, 7], division [7, 8, 13], exfoliation [14–16], and fusion [17].

In the Poiseuille type of flow, the shear rate depends on the distance from the wall: highest at the wall [14–16, 18]. In the Couette type of flow, on the other hand, the shear rate is

constant regardless of the distance from the wall [17, 19, 20].

It takes several hours for adhesion of cells to the scaffold. The effect of the shear flow depends on the alignment of the cell. At division [21] as well as at fusion, the alignment of the cell changes. Variations can be made on the alignment of cells at the timing.

In the present study, an experimental system of the Couette type flow in the constant gap with a rotating disk has been used to apply the shear stress (2 Pa) quantitatively on the myoblast during incubation at the microscopic observation *in vitro*. The behavior of each cell has been traced at division and at fusion.

2. METHODS

Couette Type of Shear Flow Device

A Couette type of shear flow device has been used in the present study: between a rotating disk and a stationary dish (Fig. 1) [19]. The medium is sheared between a rotating wall and a stationary wall. The stationary wall is the bottom of the culture dish (diameter 60 mm).

In the device, the shear rate (γ) in the medium is calculated by Eq. (1).

$$\gamma = r \omega / d \quad (1)$$

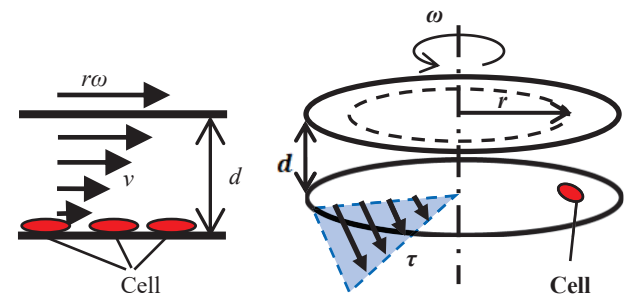


Fig. 1: Couette flow velocity (v) distribution between rotating (angular velocity ω) wall and stationary wall at r (radius) with d (distance; left): shear stress (τ) on stationary wall (right) [17].

In Eq. (1), ω is the angular velocity [rad s^{-1}], and d is the distance [m] between the wall of the moving disk and the wall of stationary plate. Between the parallel walls, d is constant in the whole space. The shear rate (γ [s^{-1}]) in the gap between walls increases in proportion to the distance (r [m]) from the rotating axis.

The angular velocity ω ($< 22 \text{ rad s}^{-1}$) was controlled by the stepping motor. In the observation area of the microscope, r varies between 17 mm and 18 mm. The distance d , which was measured by the positions of the focus of the walls at the microscope, was between 0.28 mm and 0.38 mm. Variations on the shear rates (γ) between $1 \times 10^3 \text{ s}^{-1}$ and $1.4 \times 10^3 \text{ s}^{-1}$ are made in the present experiment by adjustment of these parameters.

The shear stress (τ [Pa]) is calculated by the viscosity (η [Pa s]) of the medium.

$$\tau = \eta \gamma \quad (2)$$

Using the viscosity of the medium of $1.5 \times 10^{-3} \text{ Pa s}$ (measured by a cone and plate viscometer at 310 K), the variations of the shear stress τ have been calculated as the value between 1.5 Pa and 2.0 Pa.

The rotating disk device is mounted on the stage of the inverted phase contrast microscope placed in the incubator. The device allows the microscopic observation of cells cultured on the stationary wall during exposure to the shear flow.

Cell Culture

C2C12 (mouse myoblast cell line originated with cross-striated muscle of C3H mouse, passage between eight and ten) was used in the test. Cells were cultured in D-MEM (Dulbecco's Modified Eagle's Medium): containing 10% de complemented FBS (fetal bovine serum), sodium hydrogen carbonate (NaHCO_3), and 1% penicillin/ streptomycin.

The cells were seeded on the dish at the density of 3000 cells/ cm^2 . To make adhesion of cells to the bottom of the culture dish, the cells were cultured for 24 hours in the incubator without flow stimulation (without rotation of the disk).

After the incubation for 24 hours, the cells were continuously sheared with the rotating disk for 7 days in the incubator at the constant rotating speed without the medium exchange. The constant speed was preset for each test to keep the designed shear stress.

Measurement of Cell

The time-lapse microscopic image was taken every thirty minutes during the cultivation. The contour of each cell adhered on the stationary plate of the scaffold was traced, and the projected two-dimensional area (S) at the image of each cell was calculated. The contour of each cell was approximated to ellipsoid, and the centroid of each cell was used to measure the distance (x) between cells (Fig. 2). The area ratio ($0 < R < 1$) between two cells (the couple before fusion, or after division) was calculated by Eq. (3).

$$R_s = S_1 / S_2 \quad (3)$$

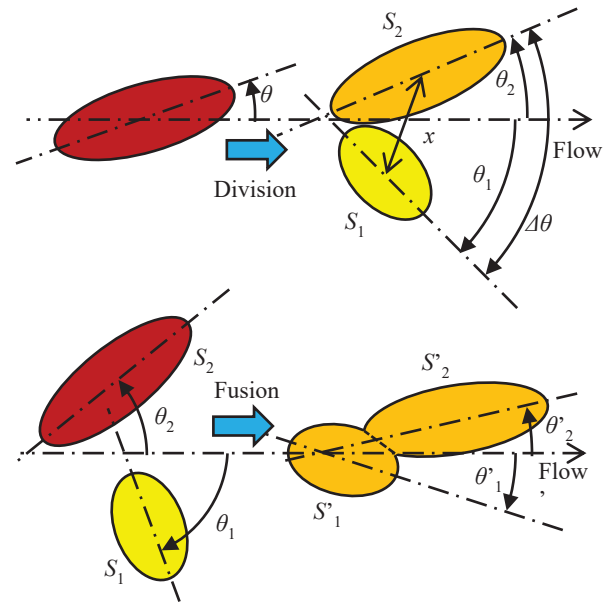


Fig. 2a: Angle (θ) between longitudinal axis of each cell and flow direction; area (S): division, and fusion.

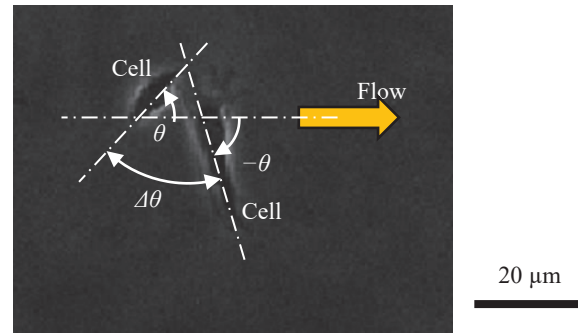


Fig. 2b: Angle (θ) between longitudinal axis of each cell and flow direction before fusion of cells.

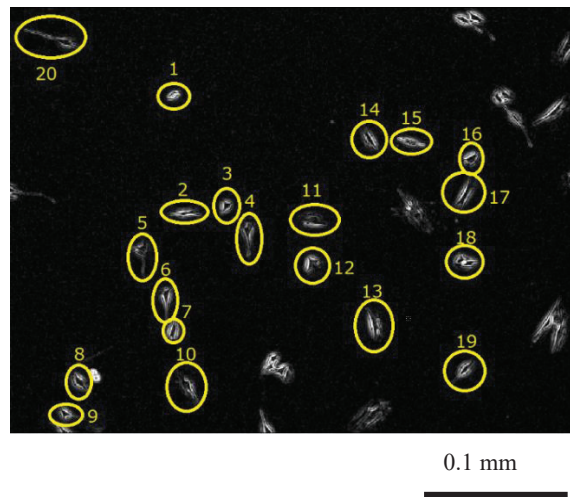


Fig. 3a: Cells (marked with each circle) traced under shear stress field of 2 Pa: flow from left to right.

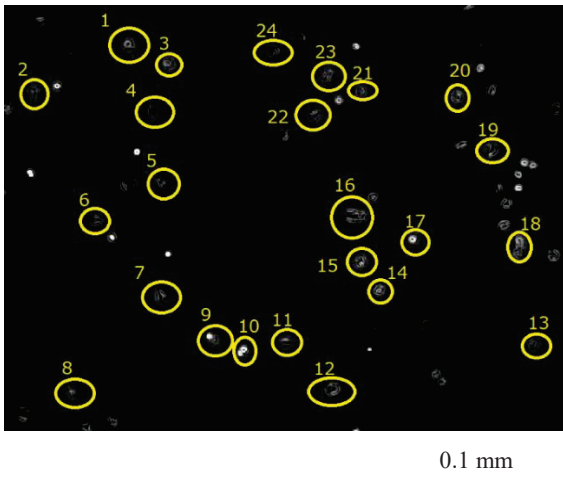


Fig. 3b: Cells (marked with each circle) traced under shear stress field of 1.5 Pa: flow from left to right.

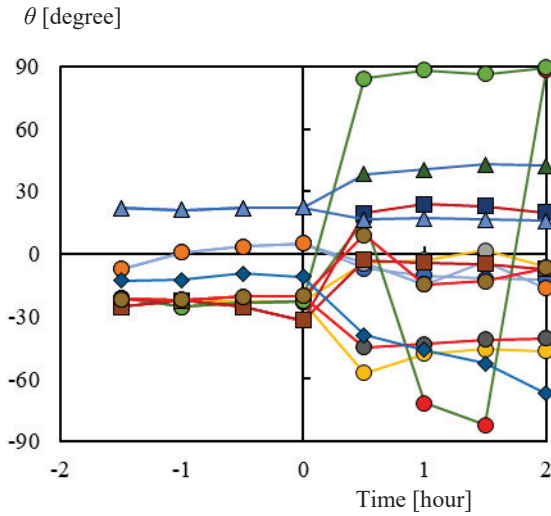


Fig. 4: Angle (θ) before and after division under shear stress field of 2 Pa: couple is shown by same marker.

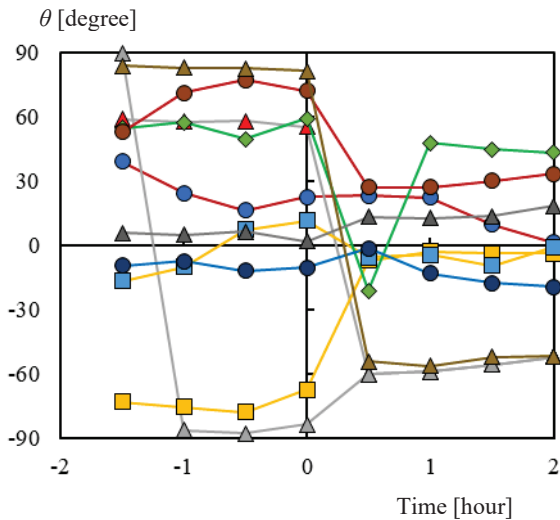


Fig. 5: Angle (θ) before and after fusion under shear stress field of 2 Pa: couple is shown by same marker.

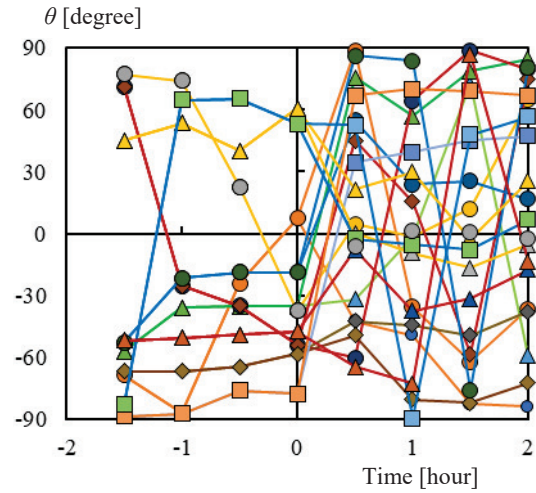


Fig. 6: Angle (θ) before and after division under shear stress field of 1.5 Pa: couple is shown by same marker.

In Eq. (3), both S_1 and S_2 are areas of “cell 1” and “cell 2”, respectively ($S_1 < S_2$). The acute angle (-90 degree $< \theta < 90$ degree) between the longitudinal axis of the cell and the flow direction was measured at the microscopic image of each cell (Fig. 2). The difference of angles between two cells (0 degree $< \Delta\theta < 90$ degree) was also measured.

3. RESULTS

Fig. 3 exemplifies images picked up from time-lapse images of cells under the shear stress field: 2 Pa in Fig. 3a, and 1.5 Pa in Fig. 3b, respectively. The behavior of each cell was traced easily by the time-lapse images every thirty minutes under shear stress field. The flow direction is from left to right in Fig. 3.

Fig. 4 shows the angle (θ) before and after division under the shear stress field of 2 Pa. The time zero corresponds to the timing of division of each cell. The negative time corresponds to the time before cell division. The direction of each cell changes at the division. The same marker corresponds to tracings of each cell. Same color of line shows tracings of related cells after division. In many cases, cells align separately after division each other. In the case of cells of the parallel direction to the flow before division, some cells tilt to the direction perpendicular to the flow after division. In Fig. 4, every cell distributes in the direction range parallel to the flow (-30 degree $< \theta < 30$ degree) before division. The angle of 90 degree corresponds to the same alignment as that of -90 degree.

Fig. 5 shows the angle (θ) before and after fusion under the shear stress field of 2 Pa. Several cells tilt to the flow direction after fusion. The alignment distribution of cells is concentrated to the parallel direction (-30 degree $< \theta < 30$ degree) after fusion. Each cell keeps its own alignment for several hours even after fusion.

Fig. 6 shows angle (θ) before and after division under shear stress field of 1.5 Pa. Under the shear stress field of 1.5 Pa, alignments of cell distribute widely.

Fig. 7 exemplifies the tracings of the angle ($\Delta\theta$) between two cells related to the distance (x) between two cells, after division for 5 hours under the shear stress field of 1.5 Pa. After division, cells have different alignments each other with the interaction between cells.

In Fig. 8, angles ($\Delta\theta$) between two cells are collected in relation to the distance (x) between two cells after division for 5 hours under the shear stress field of 2 Pa. The same marker corresponds to traced data of the same couple of cells after division. The dotted line shows the regression line, where the correlation coefficient is small ($r^2 = 0.05$). The cell tends to keep position parallel to the adjacent cell. The angle between cells tends to increase with the distance between cells.

In Fig. 9, angles ($\Delta\theta$) between two cells collected at the same timing as data in Fig.8 are illustrated in relation to the area ratio (R) between two cells under the shear stress field of 2 Pa. The dotted line shows the regression line, where the correlation coefficient (r^2) is 0.31. The angle ($\Delta\theta$) tends to increase with the area ratio. Several cells keep perpendicular position after division at the comparable areas.

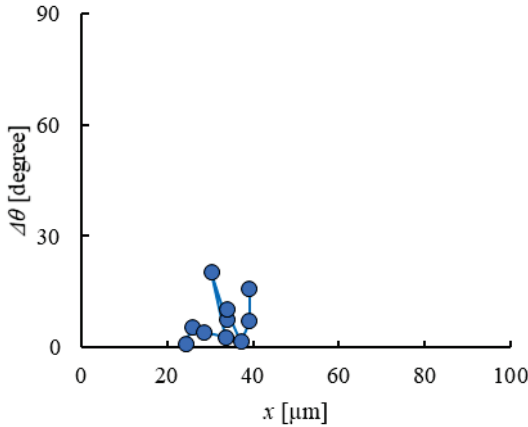


Fig. 7: Tracings of angle ($\Delta\theta$) between two cells vs. distance (x) between two cells after division for 5 hours: 1.5 Pa.

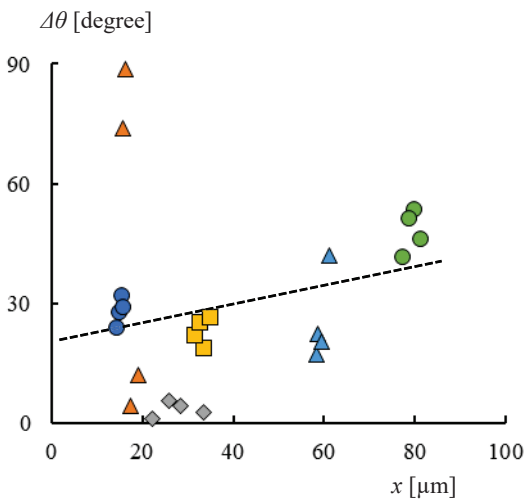


Fig. 8: Angle ($\Delta\theta$) between two cells vs. distance (x) between two cells after division for 5 hours under shear stress field of 2 Pa: $\Delta\theta = 0.21 x - 21$, $r^2 = 0.05$.

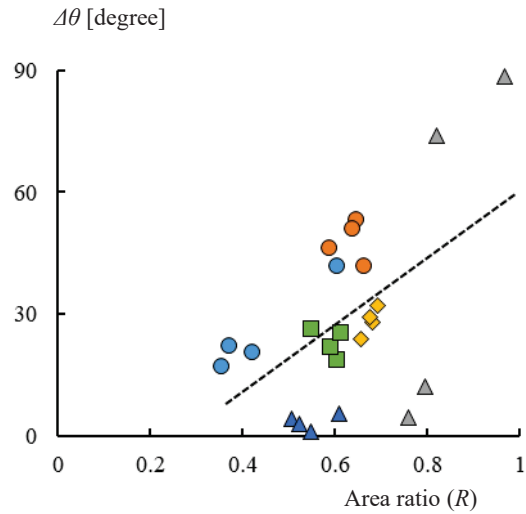


Fig. 9: Angle ($\Delta\theta$) between two cells vs. area ratio (R) between two cells after division for 5 hours under shear stress field of 2 Pa: $\Delta\theta = 89 R - 26$, $r^2 = 0.31$.

4. DISCUSSION

Endothelial cells are exposed to the shear flow in the blood vessels *in vivo*. The effect of shear flow on endothelial cells was investigated in the previous studies [1–10]. Cells are exfoliated under the shear flow at the wall shear stress higher than 2 Pa [14–16]. A biological cell shows passive and active responses in an environment [6, 22]. While the flow enhances the cell migration to the downstream, a cell migrates to adapt to the shear field. While the strong stimulation above the threshold damages the cell, the stimulation below the threshold remains in the cell as a memory for the response in the next step [5, 9]. The hysteresis effect governs the active response of the cell.

In the previous study, cells were exposed to the shear flow in a donut-shaped open channel, and the effect of flow stimulation on cultured cells has been studied *in vitro* [11, 12]. When the flow has an open surface, it is difficult to estimate the shear stress value in the fluid. Between two parallel walls, on the other hand, the velocity profile is estimated to be parabolic in the laminar flow. In the previous studies, several preparations were designed to study the effect of mechanical flow stimulations on biological cells: the tilting disk channel [14], the rhombus channel [15], the cross flow channel [16], and the rotating disk type [19].

The Couette type of flow is convenient to estimate the shear stress in the flow with the constant shear rate between the moving wall and the stationary wall, which is also available to non-Newtonian fluid. Several kinds of the devices of Couette type flow were designed for quantitative experiments of biological fluid in the previous studies [19, 20]. The cone-and-plate type device has the uniform shear field in the entire space between the rotating cone and the stationary plate [20]. The shear stress is constant independent of the distance from the rotating axis.

A parallel disks system between rotating disk and the stationary disk, on the other hand, has several advantages: stability of the rotating motion of the disk, stability of the optical path for the microscopic observation, morphologic preciseness of the plane of the disks, and simultaneous observation over the range of variation of the shear rate proportional to the radius from the rotational axis.

In the present study, the rotating parallel disk system is selected to make Couette type of flow instead of the cone and plate system. At the constant angular velocity, the shear rate ($\dot{\gamma}$) increases with the distance from the axis (r) in the observation area (Eq. (1)). The variation of the shear rate enables the simultaneous observation of the behavior of cells related to variation of the shear stress [19]. The rotating flow might induce the secondary flow by the centrifugal effect. The rotational speed of the disk is smaller than 0.4 m s^{-1} in the present system. The microscopic video image of the flowing cells between the rotating disk and the stationary disk shows the steady flow in the present experiment. Reynolds number (Re) is calculated by Eq. (4).

$$Re = \rho v d / \eta = \rho r \omega d / \eta \quad (4)$$

In Eq. (4), ρ is density of the fluid [kg m^{-3}], v is the circumferential velocity [m s^{-1}], ω is the angular velocity [rad s^{-1}], r is the distance [m] from the rotating axis, d is the distance [m] between the moving wall and the stationary wall, and η is the viscosity of the fluid [Pa s]. Re is 1×10^2 , when ρ , r , ω , d , and η are $1 \times 10^3 \text{ kg m}^{-3}$, 0.018 m , 22 rad s^{-1} , 0.00038 m , and 0.0015 Pa s , respectively. The turbulent flow may not occur in the flow of small value of Reynolds number.

In the present experiment *in vitro*, myoblasts proliferate regardless of the shear flow stimulation ($< 2 \text{ Pa}$). When myoblasts are cultured in the continuous steady shear flow without change of the medium between the plates, myoblasts differentiate to myotubes. The movement of each cell is able to be traced by the time-lapse image with the interval of thirty minutes in the present experiment.

The interaction between cells governs the behavior of each cell. The orientation of each cell depends on the orientation of the neighbor cell. The interaction decreases with the distance between cells (Fig. 8). The angle between cells tends to increase with the distance between cells. The smaller cell follows the direction of the bigger cell. The angle between cells are at random, when the sizes of the cells are comparable order (Fig. 9).

Under the shear stress field of 2 Pa , activity of each cell decreases. Some cells are exfoliated under the wall shear stress of 2 Pa . Under the shear stress field of 1.5 Pa , on the other hand, each cell at every direction makes division (Fig. 6).

Although some cells are exfoliated, differentiation of myoblast to myotube is accelerated under the wall shear stress of 2 Pa . The myoblasts tend to align to the flow direction under the shear stress field of 2 Pa . The myoblast parallel to the flow are active to make division. The number of myoblast perpendicular to the flow tends to decrease.

The shear stress field was also used to study adhesion phenomena in micro-biological systems [23]. In the previous

study, mechanical stress was studied on differentiation of stem cells [24]. Mechanical stimulation was studied on tissue formation [25]. Property of the scaffold affects differentiation of stem cells [26, 27]. Orientation of cells can be controlled by design of the scaffold [28]. Mechanism to make orientation in the tissue might be analyzed by the study on the tracings of the alignment of each cell during division and fusion [29, 30].

5. CONCLUSION

The effect of shear stress on myoblast has been investigated under the uniform shear flow *in vitro*. Couette type of shear flow field was made between a lower stationary culture plate and an upper rotating parallel plate. The wall shear stress (τ) was continuously applied on C2C12 (mouse myoblast cell line) for 7 days, and the behavior of each cell was traced at the time-lapse image observed by an inverted phase contrast microscope placed in an incubator. The experimental results show that cells make both division and fusion under shear stress $< 2 \text{ Pa}$. Interaction between divided cells decreases with the distance between cells. The smaller cell tends to follow the bigger cell related to the alignment.

ACKNOWLEDGMENT

The authors thank to Mr. Hiroki Eri for his assistance of the experiment.

REFERENCES

- [1] N. Sakamoto and N. Saito, "Effect of Spatial Gradient in Fluid Shear Stress on Morphological Changes in Endothelial Cells in Response to Flow", **Biochemical and Biophysical Research Communications**, Vol. 395, 2010, pp. 264–269.
- [2] N. Kataoka, S. Ujita and M.Sato, "Effect of Flow Direction on the Morphological Responses of Cultured Bovine Aortic Endothelial Cells", **Medical & Biological Engineering & Computing**, Vol. 36, 1998, pp. 122–128.
- [3] N. DePaola, M.A. Gimbrone Jr., P.F. Davies and C.F. Dewey Jr., "Vascular Endothelium Responds to Fluid Shear Stress Gradients", **Arteriosclerosis Thrombosis and Vascular Biology**, Vol 12, No 11, 1992, pp. 1254–1257.
- [4] M.J. Levesque and R.M. Nerem, "The Elongation and Orientation of Cultured Endothelial Cells in Response to Shear Stress", **Journal of Biomechanical Engineering**, Vol. 107, No. 4, 1985, pp. 341–347.
- [5] R. Steward Jr, D. Tambe, C.C. Hardin, R. Krishnan and J.J. Fredberg, "Fluid Shear, Intercellular Stress, and Endothelial Cell Alignment", **American Journal of Physiology–Cell Physiology**, Vol. 308, 2015, C657–C664.
- [6] M.A. Ostrowski, N.F. Huang, T.W. Walker, T. Verwijlen, C. Poplawski, A.S. Khoo, J.P. Cooke, G.G. Fuller and A.R. Dunn, "Microvascular Endothelial Cells Migrate Upstream and Align Against the Shear Stress Field Created by Impinging Flow", **Biophysical Journal**, Vol. 106, No. 2, 2014, pp. 366–374.
- [7] Y. Tardy, N. Resnick, T. Nagel, M.A. Gimbrone Jr and C.F. Dewey Jr, "Shear Stress Gradients Remodel Endothelial Monolayers in Vitro via a Cell Proliferation-Migration-Loss Cycle", **Arteriosclerosis Thrombosis and Vascular Biology**, Vol. 17, No. 11, 1997, pp. 3102–3106.
- [8] C.R. White, M. Haidekker, X. Bao and J.A. Frangos,

- “Temporal Gradients in Shear, But Not Spatial Gradients, Stimulate Endothelial Cell Proliferation”, **Circulation**, Vol. 103, 2001, pp. 2508–2513.
- [9] T. Nagel, N. Resnick, W.J. Atkinson, C.F. Dewey Jr and M. A. Gimbrone Jr, “Shear Stress Selectively Upregulates Intercellular Adhesion Molecule-1 Expression in Cultured Human Vascular Endothelial Cells”, **The Journal of Clinical Investigation**, Vol. 94, No. 2, 1994, pp. 885–891.
- [10] R.H.W. Lam, Y. Sun, W. Chen and J. Fu, “Elastomeric Microposts Integrated into Microfluidics for Flow-mediated Endothelial Mechanotransduction Analysis”, **Lab on Chip**, Vol. 12, No. 10, 2012, pp. 1865–1873.
- [11] M. Ochiai, S. Hashimoto and Y. Takahashi, “Effect of Flow Stimulation on Cultured Osteoblast”, **Proc. 18th World Multi-Conference on Systemics Cybernetics and Informatics**, Vol. 2, 2014, pp. 156–161.
- [12] S. Hashimoto and M. Okada, “Orientation of Cells Cultured in Vortex Flow with Swinging Plate In Vitro”, **Journal of Systemics Cybernetics and Informatics**, Vol. 9, No. 3, 2011, pp. 1–7.
- [13] W. Yu, H. Qu, G. Hu, Q. Zhang, K. Song, H. Guan, T. Liu and J. Qin, “A Microfluidic-based Multi-shear Device for Investigating the Effects of Low Fluid-induced Stresses on Osteoblasts”, **PLoS ONE**, Vol. 9, No. 2, 2014, pp. 1–7.
- [14] S. Hashimoto, F. Sato, H. Hino, H. Fujie, H. Iwata and Y. Sakatani, “Responses of Cells to Flow In Vitro”, **Journal of Systemics Cybernetics and Informatics**, Vol. 11, No. 5, 2013, pp. 20–27.
- [15] F. Sato, S. Hashimoto, T. Yasuda and H. Fujie, “Observation of Biological Cells in Rhombus Parallelepiped Flow Channel”, **Proc. 17th World Multi-Conference on Systemics Cybernetics and Informatics**, Vol. 1, 2013, pp. 25–30.
- [16] H. Hino, S. Hashimoto, Y. Takahashi and S. Nakano, “Design of Cross Type of Flow Channel to Control Orientation of Cell”, **Proc. 20th World Multi-Conference on Systemics Cybernetics and Informatics**, Vol. 2, 2016, pp. 117–122.
- [17] Y. Endo, S. Hashimoto and H. Eri, “Effect of Shear Stress on Myoblasts Cultured under Couette Type of Shear Flow between Parallel Disks”, **Proc. 11th International Multi-Conference on Complexity Informatics and Cybernetics**, Vol. 2, 2020, pp. 1–6.
- [18] T.H. Kim, J.M. Lee, C.D. Ahrberg and B.G. Chung, “Development of the Microfluidic Device to Regulate Shear Stress Gradients”, **BioChip Journal**, Vol. 12, No. 4, 2018, pp. 294–303.
- [19] H. Hino, S. Hashimoto, Y. Takahashi and M. Ochiai, “Effect of Shear Stress in Flow on Cultured Cell: Using Rotating Disk at Microscope”, **Journal of Systemics, Cybernetics and Informatics**, Vol. 14, No. 4, 2016, pp. 6–12.
- [20] S. Hashimoto, H. Sugimoto and H. Hino, “Behavior of Cell in Uniform Shear Flow Field between Rotating Cone and Stationary Plate”, **Journal of Systemics Cybernetics and Informatics**, Vol. 16, No. 2, 2018, pp. 1–7.
- [21] S. Hashimoto, K. Shimada and Y. Endo, “Migration of Cell under Couette Type Shear Flow Field between Parallel Disks: After and Before Proliferation”, **Proc. 11th International Multi-Conference on Complexity Informatics and Cybernetics**, Vol. 2, 2020, pp. 19–24.
- [22] F. Kurth, A. Franco-Obregon, M. Casarosa, S.K. Kuester, Karin Wuertz-Kozak and Petra S. Dittrich, “Transient Receptor Potential Vanilloid 2-mediated Shear-stress Responses in C2C12 Myoblasts Are Regulated by Serum And Extracellular Matrix”, **The FASEB Journal**, Research Communication, Vol. 29, No. 11, 2015, pp. 4726–4737.
- [23] L. Wang, R. Keatch, Q. Zhao, J.A. Wright, C.E. Bryant, A.L. Redmann and E.M. Terentjev, “Influence of Type I Fimbriae and Fluid Shear Stress on Bacterial Behavior and Multicellular Architecture of Early *Escherichia coli* Biofilms at Single-Cell Resolution”, **Applied and Environmental Microbiology**, Vol. 84, No. 6, 2018, pp. 1–13.
- [24] Y. Xie, X. Liu, S. Wang, M. Wang and G. Wang, “Proper Mechanical Stimulation Improve the Chondrogenic Differentiation of Mesenchymal Stem Cells: Improve the Viscoelasticity and Chondrogenic Phenotype”, **Biomedicine and Pharmacotherapy**, Vol. 115, No. 108935, 2019, pp. 1–5.
- [25] K.W. Aguilar-Agon, A.J. Capel, N.R.W. Martin, D.J. Player and M.P. Lewis, “Mechanical Loading Stimulates Hypertrophy in Tissue-engineered Skeletal Muscle: Molecular and Phenotypic Responses,” **Journal of Cellular Physiology**, Vol. 234, 2019, pp. 23547–23558.
- [26] H. Yuan, Y. Zhou, M.S. Lee, Y. Zhang and W.J. Li, “A Newly Identified Mechanism Involved in Regulation of Human Mesenchymal Stem Cells by Fibrous Substrate Stiffness”, **Acta Biomaterialia**, Vol. 42, 2016, pp. 247–257.
- [27] M. Werner, S.B.G. Blanquer, S.P. Haimi, G. Korus, J.W.C. Dunlop, G.N. Duda, D.W. Grijpma and A. Petersen, “Surface Curvature Differentially Regulates Stem Cell Migration and Differentiation via Altered Attachment Morphology and Nuclear Deformation”, **Advanced Science**, Vol. 4, No. 2, 2017, 1600347.
- [28] I.A.E.W. Van Loosdregt, S. Dekker, P.W. Alford, C.W.J. Oomens, S. Loerakker and C.V.C. Bouten, “Intrinsic Cell Stress is Independent of Organization in Engineered Cell Sheets,” **Cardiovascular Engineering and Technology**, Vol. 9, No. 2, 2018, pp. 181–192.
- [29] D.L. Yamamoto, R.I. Csikasz, Y. Li, G. Sharma, K. Hjort, R. Karlsson and T. Bengtsson, “Myotube Formation on Micro-patterned Glass: Intracellular Organization and Protein Distribution in C2C12 Skeletal Muscle Cells”, **Journal of Histochemistry and Cytochemistry**, Vol. 56, No. 10, 2008, pp. 881–892.
- [30] A. Patel, Y. Xue, S. Mukundan, L.C. Rohan, V. Sant, D.B. Stolz and S. Sant, “Cell-Instructive Graphene-Containing Nanocomposites Induce Multinucleated Myotube Formation”, **Annals of Biomedical Engineering**, Vol. 44, No. 6, 2016, pp. 2036–2048.